ISSN 2035-911X

International Journal of
Energy & Technology
www.journal-enertech.eu

International Journal of Energy & Technology 6 (2) (2014) 1– 9

NATURAL CONVECTION FLOW ACROSS A NANOFLUID LAYER WITH TEMPERATURE-DEPENDENT THERMAL CONDUCTIVITY AND VISCOSITY

Rehena Nasrin[1,*], M.A. Alim[1] and A.J. Chamkha[2]

[1]Department of Mathematics, Bangladesh University of Engineering and Technology, Dhaka - 1000, Bangladesh, [*]Corresponding Author, E-mail: rehena@math.buet.ac.bd

[2]Manufacturing Engineering Department, The Public Authority for Applied Education and Training, Shuweikh 70654, Kuwait

ABSTRACT

The influences of variable thermal conductivity and viscosity depended on temperature across a horizontal thin nanofluid layer is investigated numerically. The water based nanofluid with copper nanoparticles is used as the working fluid inside the layer. The governing partial differential equations with proper boundary conditions are solved by Finite Element Method using Galerkin's weighted residual scheme with discretization by triangular mesh elements. The effects temperature dependent thermal conductivity and viscosity related to performance such as temperature and velocity distributions, heat transfer, mean temperature and velocity of the nanofluid are investigated systematically. The results show that the better performance of heat transfer inside the nanofluid layer is found by using the highest and lowest values of variable thermal conductivity and viscosity respectively.

Keywords: Natural convection, nanofluid layer, finite element method, variable thermal conductivity and viscosity.

1. INTRODUCTION

The fluids with solid-sized nanoparticles suspended in them are called "nanofluids". The natural convection in enclosures continues to be a very active area of research during the past few decades. Due to small sizes and very large specific surface areas of the nanoparticles, nanofluids have superior properties like high thermal conductivity, minimal clogging in flow passages, long-term stability, and homogeneity. Applications of nanoparticles in thermal field are to enhance heat transfer from solar collectors to storage tanks, to improve efficiency of coolants in transformers. Convection is the process of heat transfer through a fluid (air, water, any fluid). One location heats the fluid, which then carries this thermal energy (higher temp fluid) to another location. Natural convection in enclosure is of vast interest of the phenomenon in many technological processes, such as the design of solar collectors, thermal design of buildings, air conditioning and the cooling of electronic circuit boards.

In physics, thermal conductivity is the intensive property of fluid that indicates its ability to conduct heat. It is evaluated primarily in terms of Fourier's Law for heat conduction. The reciprocal of thermal conductivity is called thermal resistivity. The viscosity of a fluid is a measure of its resistance to gradual deformation by shear stress or tensile stress. For liquids, it corresponds to the informal notion of "thickness". Viscosity is due to friction between neighboring parcels of the fluid that are moving at different velocities. It is the measure of the internal friction of a fluid. This friction becomes apparent when a layer of fluid is made to move in relation to another layer. The greater the friction, the greater the amount of force required to cause this movement, which is called shear. Shearing occurs whenever the fluid is physically moved or distributed, as in pouring, spreading, spraying, mixing, etc. Viscosity is a principal parameter when any flow measurements of fluids, such as liquids, semi-solids, gases and even solids are made.

Thermal conductivity and viscosity are very important properties in nanofluid heat transfer mechanism. Thermal conductivity and viscosity of fluids are temperature dependent. The fluids that have been traditionally used for heat transfer applications have a rather low thermal conductivity, taking into account the rising demands of modern technology. Thus, there is a need to develop new types of fluids that will be more effective in terms of heat exchange performance. In order to achieve this, it has been recently proposed to disperse small amounts of nanometer-sized solids in the fluid. The resulting "nanofluid" is a multiphase material that is macroscopically uniform.

Stasiek [1] made experimental studies of heat transfer and fluid flow across corrugated and undulated heat exchanger surfaces. Noorshahi et al. [2] studied numerically the natural convection effect in a corrugated enclosure with mixed boundary conditions. An innovative idea is to suspend

ultra fine solid particles in the fluid for improving the thermal conductivity of the fluid by Hetsroni and Rozenblit [3]. These early studies, however, used suspensions of millimeter- or micrometer-sized particles, which, although showed some enhancement, experienced problems such as poor suspension stability and hence channel clogging, which are particularly serious for systems using mini sized and micro sized particles. The suspended metallic or nonmetallic nanoparticles change the transport properties and heat transfer characteristics of the base fluid. Hwang et al. [4] studied the stability and thermal conductivity characteristics of nanofluids. In this study, they concluded that the thermal conductivity of ethylene glycol was increased by 30%. Kent [5] studied laminar natural convection in isosceles triangular enclosures for cold base and hot inclined walls numerically.

Parvin et al. [6] analyzed thermal conductivity variation of water-alumina nanofluid in an annulus where two thermal conductivity models namely, the Chon et al. model and the Maxwell Garnett model, are used to evaluate the heat transfer enhancement in the annulus. Roslan et al. [7] investigated heat transfer in a naonofluid filled trapezoidal enclosure with variable thermal conductivity and viscosity. They found that the effect of the viscosity was more dominant than the thermal conductivity, and there was almost no improvement in heat transfer performance utilizing nanofluids. Effects of variable viscosity and thermal conductivity of CuO-water nanofluid on heat transfer enhancement was analyzed by Abu-Nada [8]. Molla, et al. [9] studied the effect of temperature dependent viscosity on MHD natural convection flow from an isothermal sphere. They solved governing boundary layer equations numerically by two very efficient methods, namely, (i) Implicit finite difference method together with Keller box scheme and (ii) Direct numerical scheme. Hollands et al. [10] experimentally investigated free convection heat transfer across inclined air layers where a recommended relationship giving the Nusselt number as a function of Ra $\cos\phi$ and ϕ was reported.

Measurement of temperature-dependent thermal conductivity and viscosity of TiO_2-water nanofluids was conducted by Duangthongsuk and Wongwises [11]. The result showed that thermal conductivity of nanofluids increased with increasing nanofluid temperatures and, conversely, the viscosity of nanofluids decreased with increasing temperature of nanofluids. Berg et al. [12] studied the combined influences of variable thermal conductivity, temperature- and pressure-dependent viscosity and core–mantle coupling on thermal evolution. The initial value of the core–mantle boundary temperature could be inferred to wield a strong influence on the subsequent mantle thermal evolution in this model with both variable thermal conductivity and viscosity. Salem and Odda [13] investigated influence of thermal conductivity and variable viscosity on the flow of a micropolar fluid past a continuously moving plate with suction or injection. They presented their numerical results for the distribution of velocity, microrotation and temperature profiles within the boundary layer.

Effects of variable viscosity and thermal conductivity on MHD flow past a vertical plate was analyzed by Hazarika and Gopal [14]. The effects of variable viscosity and thermal conductivity on velocity profile, temperature profile and concentration profiles were investigated by solving the governing transformed ordinary differential equations with the help of Runge-Kutta shooting method. Ozalp [15] studied entropy generation for nonisothermal fluid flow with variable thermal conductivity and viscosity. Discretization was performed using a pseudospectral technique based on Chebyshev polynomial expansions. The resulting nonlinear, coupled boundary value problem was solved iteratively using Chebyshev-pseudospectral method.

Mahanti and Gaur [16] conducted effects of varying viscosity and thermal conductivity on steady free convective flow and heat transfer along an isothermal vertical plate in the presence of heat sink. Effects of variable thermal conductivity and heat source / sink on MHD flow near a stagnation point on a linearly stretching sheet was showed by Sharma and Singh [17]. The equations of continuity, momentum and energy were transformed into ordinary differential equations and solved numerically using shooting method. Choudhury and Hazarika [18] studied the effects of variable viscosity and thermal conductivity on MHD flow due to a point sink. Results showed that the effects of the variable thermo-viscous parameters and magnetic parameter were considerable and they had to be taken into consideration in the flow and heat transfer problem.

Nasrin [19] studied influences of physical parameters on mixed convection in a horizontal lid driven cavity with undulating base surface. Combined convection flow in triangular wavy chamber filled with water-CuO nanofluid with viscosity models variation was investigared by Nasrin, et al. [20]. Two different nanofluid models namely, the Brinkman model and the Pak and Cho correlation were employed. The developed equations were given in terms of the Navier Stokes and the energy equation and were non-dimensionalized and then solved numerically subject to appropriate boundary conditions by the Galerkin's finite-element method.

From the literature review it is mentioned that a very few numerical works have been done introducing temperature dependent thermal conductivity and viscosity properties of nanofluid. In spite of that there is a large scope to work with nanofluid flow and heat transfer by analyzing these two properties. In this paper, we investigate numerically the effect of variable thermal conductivity and viscosity across the nanofluid layer having sinusoidal-wave at bottom. So, the objective of this article is to present flow and heat transfer phenomena of water/Cu nanofluid due to the thermal conductivity and viscosity variation inside a thin layer.

2. PHYSICAL MODELING

Fig. 1 shows a schematic diagram of a nanofluid layer. This layer is filled by water-based nanofluid containing Cu nanoparticles. The nanofluid is assumed incompressible and the flow is considered to be laminar. It is considered that water and Cu nanoparticles are in thermal equilibrium and no slip occurs among them. It is assumed that the Cu nanoparticles are spherical shaped and diameters are less than 10nm. The bottom wavy wall is maintained uniformly with constant temperature T_c whereas the top surface is

heated by temperature T_w (T_w>T_c). The vertical walls are perfectly insulated. The density of the nanofluid is approximated by the Boussinesq model. Amplitude of wave A_m = 0.04 and number of wave λ = 3.5 are assumed. L and H are respectively the length and average height of considered domain.

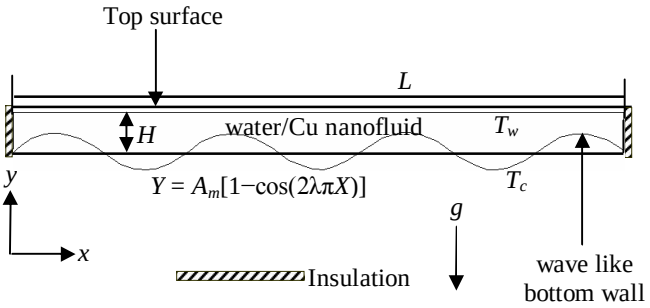

Fig. 1: Schematic diagram of the nanofluid layer

2.1. MATHEMATICAL MODELING

The governing equations for steady laminar natural convection across a nanofluid layer in terms of the Navier-Stokes and energy equation (dimensional form) with temperature dependent thermal conductivity and viscosity are equation (dimensional form) are taken from Lin and Violi [21] and given as:

Continuity equation:

$$\frac{\partial u}{\partial x}+\frac{\partial v}{\partial y}=0 \tag{1}$$

x-momentum equation:

$$\rho_{nf}\left(u\frac{\partial u}{\partial x}+v\frac{\partial u}{\partial y}\right)=-\frac{\partial p}{\partial x}+\left[\frac{\partial}{\partial x}\left(\mu_{nf}\frac{\partial u}{\partial x}\right)+\frac{\partial}{\partial y}\left(\mu_{nf}\frac{\partial u}{\partial y}\right)\right] \tag{2}$$

y-momentum equation:

$$\rho_{nf}\left(u\frac{\partial v}{\partial x}+v\frac{\partial v}{\partial y}\right)=-\frac{\partial p}{\partial y}+\left[\frac{\partial}{\partial x}\left(\mu_{nf}\frac{\partial v}{\partial x}\right)+\frac{\partial}{\partial y}\left(\mu_{nf}\frac{\partial v}{\partial y}\right)\right]+g\left(\rho\beta\right)_{nf}(T-T_c) \tag{3}$$

Energy equation:

$$u\frac{\partial T}{\partial x}+v\frac{\partial T}{\partial y}=\frac{1}{\left(\rho C_p\right)_{nf}}\left[\frac{\partial}{\partial x}\left(k_{nf}\frac{\partial T}{\partial x}\right)+\frac{\partial}{\partial y}\left(k_{nf}\frac{\partial T}{\partial y}\right)\right] \tag{4}$$

where, $\rho_{nf}=(1-\phi)\rho_f+\phi\rho_s$ is the density,

$\left(\rho C_p\right)_{nf}=(1-\phi)\left(\rho C_p\right)_f+\phi\left(\rho C_p\right)_s$ is the heat capacitance,

$\beta_{nf}=(1-\phi)\beta_f+\phi\beta_s$ is the thermal expansion coefficient,

$\alpha_{nf}=k_{nf}\left/\left(\rho C_p\right)_{nf}\right.$ is the thermal diffusivity,

In the current study, the effective viscosity of the nanofluid is considered by the Brinkman model [22]

$$\mu_{nf}=\mu_f(1-\phi)^{-2.5}$$

Also the effective thermal conductivity is used from Maxwell Garnett (MG) model [23]

$$k_{nf}=k_f\frac{\left(k_s+k_s\right)+2k_f-2\phi\left(k_f-k_s\right)}{\left(k_s+k_s\right)+2k_f+\phi\left(k_f-k_s\right)}.$$

Consider the temperature dependent thermal conductivity, which is proposed by Charraudeau [24], as follows

$$k=k_\infty[1+\delta(T-T_c)]=\kappa_{nf}\ (\text{Let}) \tag{5}$$

where k_∞ is the thermal conductivity of the ambient fluid and $\delta=\frac{1}{\kappa}\left(\frac{\partial\kappa}{\partial T}\right)$ is a constant.

There are very few forms of viscosity variation available in the literature. Among them one is considered here which is appropriate for liquid introduced by Hossain et al. [25] as follows:

$$\mu=\mu_\infty[1+\chi(T-T_c)]=\mu_{nf}\ (\text{Let}) \tag{6}$$

where μ_∞ is the viscosity of the ambient fluid and $\chi=\frac{1}{\mu}\left(\frac{\partial\mu}{\partial T}\right)$ is a constant evaluated at the film temperature of the flow $T_{fl}=\frac{1}{2}\left(T_w+T_c\right)$.

The boundary conditions are:

at all solid boundaries: $u = v = 0$
at the top surface: $T = T_w$
at the vertical walls: $\frac{\partial T}{\partial x}=0$
at the bottom wavy surface: $T = T_c$

The above equations are non-dimensionalized by using the following dimensionless dependent and independent variables:

$$X=\frac{x}{L},\quad Y=\frac{y}{L},\quad U=\frac{uL}{\nu_f},\quad V=\frac{vL}{\nu_f},$$

$$P=\frac{pL^2}{\rho_f{\nu_f}^2},\quad \theta=\frac{T-T_c}{T_w-T_c}$$

Then the non-dimensional governing equations are

$$\frac{\partial U}{\partial X}+\frac{\partial V}{\partial Y}=0 \tag{7}$$

$$U\frac{\partial U}{\partial X}+V\frac{\partial U}{\partial Y}=-\frac{\rho_f}{\rho_{nf}}\frac{\partial P}{\partial X}+\frac{(1+\eta\theta)}{\rho_{nf}}\left(\frac{\partial^2U}{\partial X^2}+\frac{\partial^2U}{\partial Y^2}\right)+\frac{\eta}{\rho_{nf}}\left(\frac{\partial\theta}{\partial X}\frac{\partial U}{\partial X}+\frac{\partial\theta}{\partial Y}\frac{\partial U}{\partial Y}\right) \tag{8}$$

$$U\frac{\partial V}{\partial X}+V\frac{\partial V}{\partial Y} = -\frac{\rho_f}{\rho_{nf}}\frac{\partial P}{\partial Y}+\frac{(1+\eta\theta)}{\rho_{nf}}\left(\frac{\partial^2 V}{\partial X^2}+\frac{\partial^2 V}{\partial Y^2}\right)+ \frac{\eta}{\rho_{nf}}\left(\frac{\partial\theta}{\partial X}\frac{\partial V}{\partial X}+\frac{\partial\theta}{\partial Y}\frac{\partial V}{\partial Y}\right)+\frac{Ra}{Pr}\frac{(1-\phi)(\rho\beta)_f+\phi(\rho\beta)_s}{\rho_{nf}\beta_f}\theta \quad (9)$$

$$u\frac{\partial\theta}{\partial x}+v\frac{\partial\theta}{\partial y} = \frac{1}{Pr}\frac{1}{\alpha_f(\rho C_p)_{nf}}(1+\gamma\theta)\left(\frac{\partial^2\theta}{\partial X^2}+\frac{\partial^2\theta}{\partial Y^2}\right) \frac{1}{Pr}\frac{1}{\alpha_f(\rho C_p)_{nf}}\gamma\left\{\left(\frac{\partial\theta}{\partial X}\right)^2+\left(\frac{\partial\theta}{\partial Y}\right)^2\right\} \quad (10)$$

where $Pr=\frac{\nu_f}{\alpha_f}$ is the Prandtl number, $Ra=\frac{g\beta_f L^3(T_w-T_c)}{\nu_f\alpha_f}$ is the Rayleigh number, $\gamma=\delta(T_w-T_c)$ is the dimensionless thermal conductivity variation parameter and $\eta=\chi(T_w-T_c)$ is the dimensionless viscosity variation parameter.

The corresponding boundary conditions take the following form:

at all solid boundaries: $U = V = 0$

at the vertical walls: $\frac{\partial\theta}{\partial X}=0$

at the bottom surface: $\theta = 0$

at the top boundary: $\theta = 1$

The shape of the bottom wavy surface is assumed to mimic the following pattern $Y=A_m[1-\cos(2\lambda\pi X)]$ where A_m is the dimensionless amplitude of the wavy surface and λ is the number of undulations.

2.2 Average Nusselt number

The average Nusselt number (*Nu*) is expected to depend on a number of factors such as thermal conductivity, heat capacitance, viscosity, flow structure of nanofluids, volume fraction, dimensions and fractal distributions of nanoparticles.

The non-dimensional form of local heat transfer at the top surface is $\overline{Nu}=-\frac{k_{nf}}{k_f}\frac{\partial\theta}{\partial Y}$.

By integrating the local Nusselt number over the top heated surface, the average heat transfer along the heated wall of the nanofluid thin layer is as $Nu=\int_0^1\overline{Nu}\,dX$.

The mean bulk temperature and average sub domain velocity of the fluid inside the thin layer may be written as $\theta_{av}=\int\theta\,d\bar{V}/\bar{V}$ and $V_{av}=\int V\,d\bar{V}/\bar{V}$, where $\bar{V}$ and V are the volume of the thin layer and magnitude of the mean velocity inside the layer.

3. NUMERICAL TECHNIQUE

The Galerkin finite element method [26, 27] is used to solve the non-dimensional governing equations along with boundary conditions for the considered problem. The equation of continuity has been used as a constraint due to mass conservation and this restriction may be used to find the pressure distribution. This method is used to solve the Eqs. (8) - (10), where the pressure *P* is eliminated by a constraint ξ, and the incompressibility criteria given by equation (7) which can be expressed as

$$P=-\xi\left(\frac{\partial U}{\partial X}+\frac{\partial V}{\partial Y}\right) \quad (11)$$

The continuity equation is automatically fulfilled for large values of ξ. Then the velocity components (*U*, *V*), and temperature (θ) are expanded using a basis set $\{\Phi\}_{k=1}^N$ as

$$U\approx\sum_{k=1}^N U_k\Phi_k(X,Y), V\approx\sum_{k=1}^N V_k\Phi_k(X,Y) \text{ and } \theta\approx\sum_{k=1}^N\theta_k\Phi_k(X,Y) \quad (12)$$

The Galerkin finite element technique yields the subsequent nonlinear residual equations for the Eqs. (8), (9) and (10) respectively at nodes of the internal domain Ω:

$$R_i^{(1)}=\sum_{k=1}^N U_k\int_\Omega\left[\left(\sum_{k=1}^N U_k\Phi_k\right)\frac{\partial\Phi_k}{\partial X}+\left(\sum_{k=1}^N V_k\Phi_k\right)\frac{\partial\Phi_k}{\partial Y}\right]\Phi_i dXdY -\xi\frac{\rho_f}{\rho_{nf}}\left[\sum_{k=1}^N U_k\int_\Omega\frac{\partial\Phi_i}{\partial X}\frac{\partial\Phi_k}{\partial X}dXdY+\sum_{k=1}^N V_k\int_\Omega\frac{\partial\Phi_i}{\partial X}\frac{\partial\Phi_k}{\partial Y}dXdY\right]- \frac{1+\eta\theta}{\rho_{nf}}\sum_{k=1}^N U_k\int_\Omega\left[\frac{\partial\Phi_i}{\partial X}\frac{\partial\Phi_k}{\partial X}+\frac{\partial\Phi_i}{\partial Y}\frac{\partial\Phi_k}{\partial Y}\right]- \frac{\eta}{\rho_{nf}}\left[\sum_{k=1}^N U_k\int_\Omega\frac{\partial\Phi_k}{\partial X}\sum_{k=1}^N\theta_k\frac{\partial\Phi_k}{\partial X}+\sum_{k=1}^N U_k\int_\Omega\frac{\partial\Phi_k}{\partial Y}\sum_{k=1}^N\theta_k\frac{\partial\Phi_k}{\partial Y}\right]dXdY \quad (13)$$

$$R_i^{(2)}=\sum_{k=1}^N V_k\int_\Omega\left[\left(\sum_{k=1}^N U_k\Phi_k\right)\frac{\partial\Phi_k}{\partial X}+\left(\sum_{k=1}^N V_k\Phi_k\right)\frac{\partial\Phi_k}{\partial Y}\right]\Phi_i dXdY -\xi\frac{\rho_f}{\rho_{nf}}\left[\sum_{k=1}^N U_k\int_\Omega\frac{\partial\Phi_i}{\partial Y}\frac{\partial\Phi_k}{\partial X}dXdY+\sum_{k=1}^N V_k\int_\Omega\frac{\partial\Phi_i}{\partial Y}\frac{\partial\Phi_k}{\partial Y}dXdY\right]- \frac{1+\eta\theta}{\rho_{nf}}\sum_{k=1}^N V_k\int_\Omega\left[\frac{\partial\Phi_i}{\partial X}\frac{\partial\Phi_k}{\partial X}+\frac{\partial\Phi_i}{\partial Y}\frac{\partial\Phi_k}{\partial Y}\right] \frac{\eta}{\rho_{nf}}\left[\sum_{k=1}^N V_k\int_\Omega\frac{\partial\Phi_k}{\partial X}\sum_{k=1}^N\theta_k\frac{\partial\Phi_k}{\partial X}+\sum_{k=1}^N V_k\int_\Omega\frac{\partial\Phi_k}{\partial Y}\sum_{k=1}^N\theta_k\frac{\partial\Phi_k}{\partial Y}\right]dXdY -\frac{Ra}{Pr}\frac{(1-\phi)(\rho\beta)_f+\phi(\rho\beta)_s}{\rho_{nf}\beta_f}\int_\Omega\left(\sum_{k=1}^N\theta_k\Phi_k\right)\Phi_i dXdY \quad (14)$$

$$R_i^{(3)} = \sum_{k=1}^{N}\theta_k \int_{\Omega}\left[\left(\sum_{k=1}^{N}U_k\Phi_k\right)\frac{\partial\Phi_k}{\partial X}+\left(\sum_{k=1}^{N}V_k\Phi_k\right)\frac{\partial\Phi_k}{\partial Y}\right]\Phi_i dXdY -$$

$$\frac{1}{Pr}\frac{1}{\alpha_f\left(\rho C_p\right)_{nf}}\left[\begin{array}{l}\left(1+\gamma\theta\right)\sum_{k=1}^{N}\theta_k\int_{\Omega}\left(\frac{\partial\Phi_i}{\partial X}\frac{\partial\Phi_k}{\partial X}+\frac{\partial\Phi_i}{\partial Y}\frac{\partial\Phi_k}{\partial Y}\right)dXdY \\ +\gamma\left\{\left(\sum_{k=1}^{N}\theta_k\int_{\Omega}\frac{\partial\Phi_k}{\partial X}\right)^2+\left(\sum_{k=1}^{N}\theta_k\int_{\Omega}\frac{\partial\Phi_k}{\partial Y}\right)^2\right\}dXdY\end{array}\right] \quad (15)$$

Three points Gaussian quadrature is used to evaluate the integrals in these equations. The non-linear residual equations (13), (14) and (15) are solved using Newton–Raphson method to determine the coefficients of the expansions in Eq. (12). The convergence of solutions is assumed when the relative error for each variable between consecutive iterations is recorded below the convergence criterion ε such that $\left|\Psi^{n+1}-\Psi^{n}\right|\le 10^{-4}$, where n is the number of iteration and Ψ is a function of U, V and θ.

3.1. Mesh Generation

In finite element method, the mesh generation is the technique to subdivide a domain into a set of sub-domains, called finite elements, control volume etc. The discrete locations are defined by the numerical grid, at which the variables are to be calculated. It is basically a discrete representation of the geometric domain on which the problem is to be solved. The computational domains with irregular geometries by a collection of finite elements make the method a valuable practical tool for the solution of boundary value problems arising in various fields of engineering. Fig. 2 displays the finite element mesh of the present physical domain.

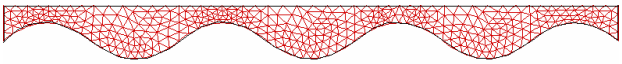

Fig. 2: Mesh generation of the nanofluid layer

3.2. Grid Independent Test

Table 1: Grid Sensitivity Check at Pr = 6.2, ϕ = 5% and Ra = 10^5

Nodes (elements)	4320 (2884)	7982 (4835)	12538 (6519)	17295 (8153)	21524 (10548)
Nu (Nanofluid)	6.82945	7.98176	8.87015	9.11216	9.195490
Nu (Base fluid)	5.62945	6.88176	7.88701	8.51556	8.61556
Time (s)	238.265	321.594	395.157	488.328	629.375

An extensive mesh testing procedure is conducted to guarantee a grid-independent solution for Pr = 6.2, Ra = 10^5 and ϕ = 5% in a nanofluid layer. In the present work, we examine five different non-uniform grid systems with the following number of elements within the resolution field: 2884, 4835, 6519, 8153 and 10548. The numerical scheme is carried out for highly precise key in the average Nusselt number *Nu* for water/Cu nanofluid and base fluid the aforesaid elements to develop an understanding of the grid fineness as shown in Table 1 and Fig. 3. The scale of the average Nusselt numbers for 8153 elements shows a little difference with the results obtained for the other elements. Hence, considering the non-uniform grid system of 8153 elements is preferred for the computation.

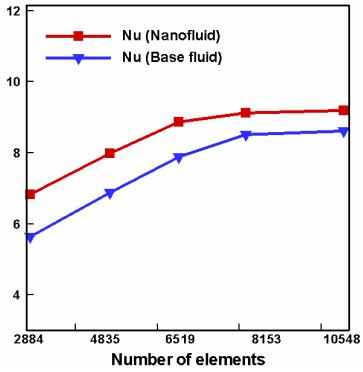

Fig. 3: Grid test for the current geometry

3.3 Thermo-physical Properties

The thermophysical properties of the Cu/water nanofluid are taken from Ogut [28] and given in Table 2.

Table 2. Thermo-physical properties of water-Cu nanofluid

Physical properties	water	Cu
C_p (J/Kg K)	4179	385
ρ (Kg/m^3)	997.1	8933
K (W/m K)	0.613	400
α x10^7 (m^2/s)	1.47	1163.1
β (K^{-1})	2.1×10^{-4}	5.1×10^{-5}

4. RESULTS AND DISCUSSION

In this section, the behavior of Cu /water nanofluid for different values of variable thermal conductivity (γ) and viscosity (η) across a nanofluid thin layer are displayed. The considered values of γ and η are γ (= 0, 1, 2 and 3) and η (= 0, 3, 6 and 10) while the Prandtl number Pr = 6.2, ϕ = 5% and Ra = 10^5 are kept fixed. In addition, the velocity and temperature fields interms of streamlines and isothermal lines, the values of the average Nusselt number, mean bulk temperature and average velocity of working fluid graphically for the pertinent parameters. For the presentation

of heat transfer rate, mean temperature and average velocity profiles the performance of water-Cu nanofluid as well as base fluid ($\phi = 0\%$) are shown in figures 8, 9 and 10.

4.1 Effect of Variable Thermal Conductivity

The effect of temperature dependent thermal conductivity (γ) on the thermal field is presented in Fig. 4 while $\eta = 0$, $\phi = 5\%$, $Pr = 6.2$ and $Ra = 10^5$. Thermal conduction is the spontaneous transfer of thermal energy through fluid, from a region of high temperature to a region of lower temperature. The strength of the thermal current activities is more activated with escalating γ. Isotherms are almost similar to the active parts for water/Cu nanofluid. Increasing γ, the temperature lines at the middle part of the nanofluid layer become horizontal whereas initially they are almost wavy pattern due to concentration of solid particles is dominated across the layer. With the rising values of thermal conductivity variation parameter γ, the temperature distributions become distorted resulting in an increase in the overall heat transfer across the thin layer.

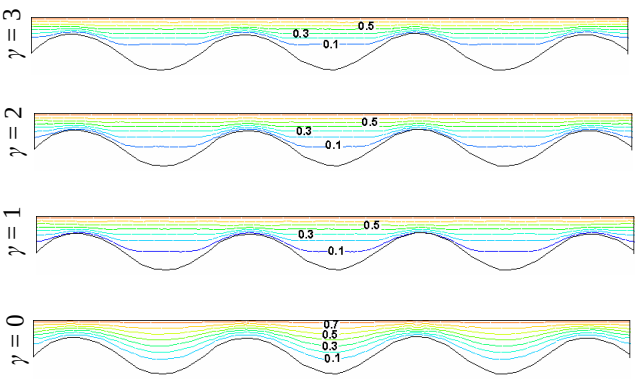

Fig. 4: Effect of γ on isothermal lines at $\eta = 0$

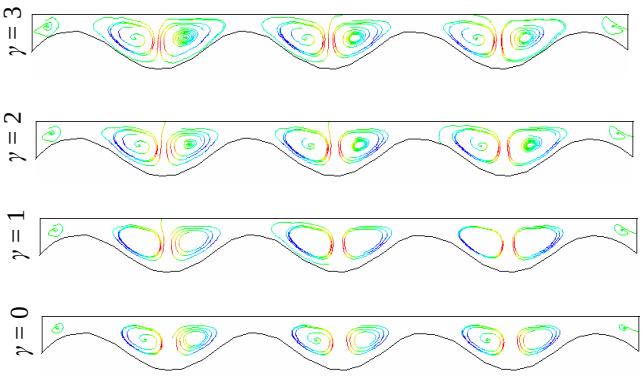

Fig. 5: Effect of γ on streamlines lines at $\eta = 0$

This result can be attributed to the dominance of the solid concentration of water-Cu nanofluid. It is worth noting that as the thermal conductivity variation of nanofluid increases, the thickness of the thermal boundary layer near the top surface enhances which indicates a steep temperature gradients and hence, an increase in the overall heat transfer from the upper wall to the wavelike bottom surface. The labeling in the isothermal lines indicates the number of lines in order.

The corresponding velocity field is depicted in Fig. 5. For water-Cu nanofluid, six primary recirculation cells occupying the whole thin layer is found at the absence of the variable thermal conductivity ($\gamma = 0$). As well as two tiny eddies appear near the left and right vertical walls in this case. In each wave, the right and left vortices rotate in counter clockwise and clockwise direction respectively. For increasing γ, velocity of working nanofluid increases and thus size of the created eddies becomes larger. In addition simple and regular characteristics are observed in the streamlines at $\gamma = 3$.

4. 2 Effect of Viscosity Variation

Fig. 6 exposes the heat transfer for various temperature dependent viscosity η (= 0-10) where $\gamma = 0$, $\phi = 5\%$, $Ra = 10^5$ and $Pr = 6.2$. In this figure it is observed that as the variable viscosity of water-Cu nanofluid enhances from 0 to 10, the isothermal contours tend to get affected considerably. In addition, these lines corresponding to $\eta = 3$ become more bended whereas initially ($\eta = 0$) the lines are horizontal at the middle of the thin layer. The isotherms tend to gather near the bottom surface of the nanofluid thin layer where the contour lines mimic the wall's profile.

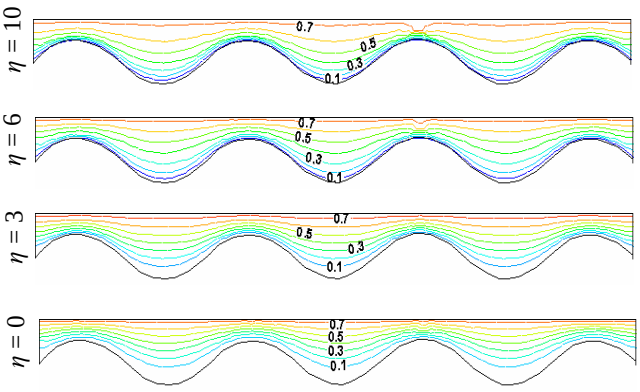

Fig. 6: Effect of η on isothermal lines at $\gamma = 0$

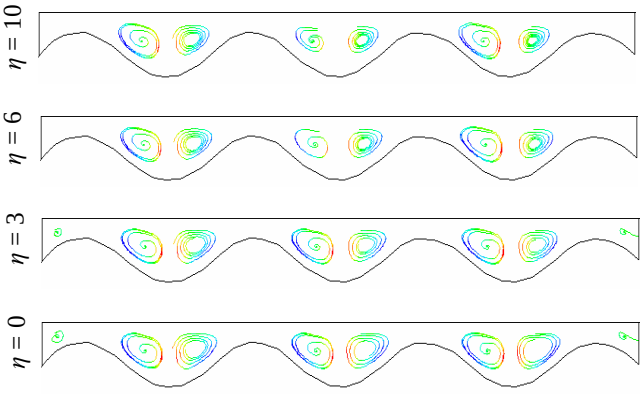

Fig. 7: Effect of η on streamlines at $\gamma = 0$

Futher rising viscosity variation parameter η leads to deformation of the thermal boundary layer at the top wall. However, the decrease in the thermal gradients at the top wall is found for the highest value of variable viscosity η = 10 of the considered nanofluid. This means that heat transfer rate diminishes due to this viscosity variation across the nanofluid layer.

The fluid flow with the variation of η is represented in the Fig. 7. The streamlines cover the entire collector in the absence of variable viscosity η forming few eddies. The change in the velocity field is not similar to the Fig. 5. In the presence of η (=1) of the water-Cu nanofluid the core of the vortices becomes slightly smaller. This is due to the fact that rising viscosity variation of the working fluid causes slower the movement of the fluid particles. At η = 6, two little eddies from the left and right corner of the nanofluid layer disappear. Finally, nanofluid motion retards significantly.

4. 3 Rate of Heat Transfer

Fig. 8 (i)-(ii) displays the average Nusselt number (*Nu*) of nanofluid and base fluid for the effect of variable thermal conductivity and viscosity respectively. Mounting thermal conductivity variation parameter γ enhances average Nusselt number. From Fig. 8(i) it is observed that rate of heat transfer enhances by 19% and 14% for nanofluid and base fluid (clear water) with the increasing values of γ from 0 to 3. Thus if it is focused on maximizing the heat transfer coefficient, it is clear that the thermal conductivity of the fluid is the dominant parameter. This is because the thermal conductivity of the solid particles is higher than the clear water (without solid particles). This means that higher heat transfer rate is predicted by the nanofluid than the base fluid (ϕ = 0%).

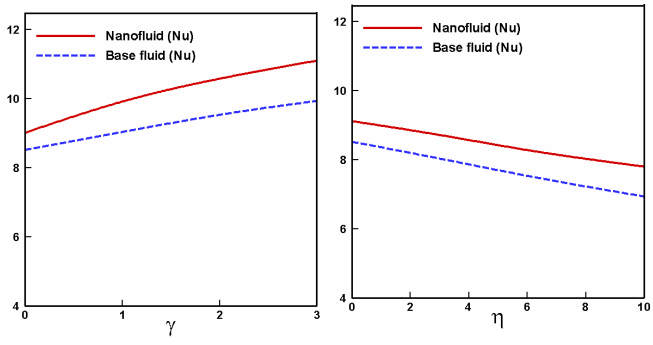

Fig. 8: Rate of heat transfer for the effect of (i) γ and (ii) η

But from Fig. 8(ii) it is seen that mean Nusselt number devalues for the variation of temperature dependent viscosity parameter η from 0 to 10. The rates of heat transfer lessen by 14% and 18% for nanofluid and base fluid respectively. The thermal conductivity of nanoparticles is higher than water. That's why decreasing rate of convective heat transfer is found lower for nanofluid than clear water.

4. 4 Mean Temperature of Fluids

The mean temperature (θ_{av}) of both type of fluids inside the thin layer for the effect of variable thermal conductivity and viscosity are displayed by the Fig. 9(i)-(ii). From this figure it is found that θ_{av} for nanofluid and base fluid grows with the rising of both parameters γ and η. As $\gamma = \delta(T_w - T_c)$, so increasing values of γ increase this temperature difference between the top and bottom surfaces. Then heat is transferred rapidly from top to bottom wall within the working fluids. That's why both velocity and temperature profiles increase with the increasing values of γ. On the other hand, for escalating viscosity variation parameter (η) the friction among fluid particles rises. As well as mean temperatures of fluids enhance. θ_{av} for nanofluid is higher in Fig. 9(i)-(ii) with compared to that of base fluid. This is due to the fact that temperature of nanofluid rises for the higher thermal conductivity of copper nanoparticles.

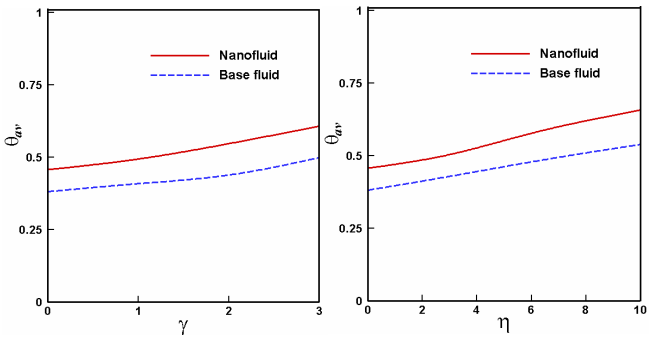

Fig. 9: Mean temperature of fluids for the effect of (i) γ and (ii) η

4. 4 Average Velocity of Fluids

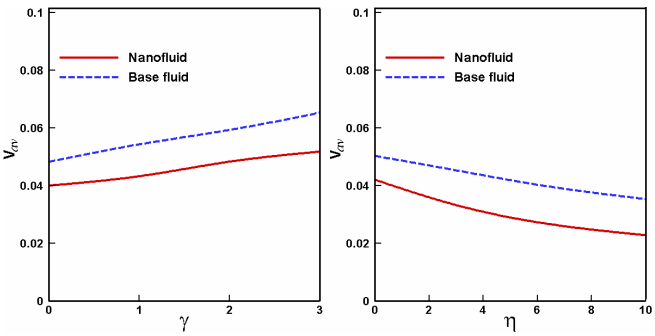

Fig. 10: Mean velocity of fluids for the effect of (i) γ and (ii) η

Fig. 10(i)-(ii) exposes the average magnitude of velocity (V_{av}) of both nanofluid and clear water in a corrugated thin nanofluid layer for the effect of thermal conductivity and viscosity variation respectively. The mean velocity has notable changes with different values of γ and η. V_{av} enhances with increasing and decreasing values of variable thermal conductivity and viscosity respectively. It is well known that movement of highly viscous fluid is slower than low viscous fluid. Here base fluid (ϕ = 0%) has higher mean velocity than the nanofluid having copper

nanoparticles. This is expected because nanofluid that is fluid with solid concentrations does not move freely like clear water.

5. CONCLUSION

The influences of temperature dependent thermal conductivity and viscosity on natural convection boundary layer flow inside a thin layer with water based nanofluid having copper nanoparticles are accounted. Various values of above mentioned variable properties have been considered for the flow and temperature fields as well as the convective heat transfer rate, mean bulk temperature of the fluids and average velocity field inside the wavy layer while Pr, ϕ and Ra are fixed at 6.2, 5% and 10^5 respectively. The results of the numerical analysis lead to the following conclusions:

- The structure of the fluid streamlines and isotherms within the thin layer is found to significantly depend upon the temperature dependent thermal conductivity.
- Water/Cu nanofluid for the absence of viscosity variation having tiny vortices in the velocity field which disappear at the higher values of η due to high viscous effect.
- The Cu nanoparticles with the highest γ and lowest η are established to be ore effective in enhancing performance of heat transfer rate across the layer.
- Mean temperature rises for nanofluid with growing γ and η.
- Magnitude of average velocity devalues due to falling thermal conductivity and growing viscosity variation.

REFERENCES

[1] JA Stasiek, Experimental studies of heat transfer and fluid flow across corrugated-undulated heat exchanger surfaces, Int. J. Heat Mass Transf., Vol. 41, pp. 899-914, 1998.

[2] S Noorshahi, CA Hall, EK Glakpe, Natural convection in a corrugated enclosure with mixed boundary conditions, ASME J. of Solar Energy Engg., Vol. 118, pp. 50-57, 1996.

[3] G Hetsroni, R Rozenblit, Heat transfer to a liquid–solid mixture in a flume, Int. J. Multiph. Flow, Vol. 20, no. 4, pp. 671–689, 1994.

[4] Y Hwang, JK Lee, CH Lee, YM Jung, SI Cheong, CG Lee, BC Ku, SP Jang, Stability and thermal conductivity characteristics of nanofluids, Thermochimica Acta, Vol. 455, No. 1–2, pp. 70–74, 2007.

[5] EF Kent, Numerical analysis of laminar natural convection in isosceles triangular enclosures for cold base and hot inclined walls, Mechanics Res. Commun., Vol. 36, pp. 497–508, 2009.

[6] S Parvin, R Nasrin, MA Alim, NF Hossain, and AJ Chamkha, Thermal conductivity variation on natural convection flow of water-alumina nanofluid in an annulus, Int. J. of Heat and Mass Transf., Vol. 55, No. 19-20, pp. 5268-5274, 2012.

[7] R Roslan, H Saleh, and I Hashim, Buoyuancy driven heat transfer in a naonofluid filled trapezoidal enclosure with variable thermal conductivity and viscosity, Num. Heat Transf., Part A: Applications, Vol. 60, No. 10, pp. 867-882, 2011.

[8] E Abu-Nada, Effects of variable viscosity and thermal conductivity of CuO-Water nanofluid on heat transfer enhancement in natural convection: Mathematical Model and Simulation, ASME J. of Heat Transf., Vol. 30, No. 4, pp. 679-690, 2009.

[9] MM Molla, SC Saha and MA Hossain, The effect of temperature dependent viscosity on MHD natural convection flow from an isothermal sphere, J. of Appl. Fluid Mech., Vol. 5, No. 2, pp. 25-31, 2012.

[10] KGT Hollands, TE Unny, GD Raithby, L. konicek, Free convection heat transfer across inclined air layers, Trans. of the American Soc. of Mech. Engineers, J. of Heat Transf., Vol. 98, pp. 189–193, 1976.

[11] W Duangthongsuk and S Wongwises, Measurement of temperature-dependent thermal conductivity and viscosity of TiO_2-water nanofluids, Exp. Thermal and Fluid Sci., Vol. 33, No. 4, pp. 706–714, 2009.

[12] AP van den Berg, ESG Rainey, DA Yuen, The combined influences of variable thermal conductivity, temperature- and pressure-dependent viscosity and core–mantle coupling on thermal evolution, Physics of the Earth and Planetary Interiors, Vol. 149, pp. 259-278, 2005.

[13] AM Salem and SN Odda, influence of thermal conductivity and variable viscosity on the flow of a micropolar fluid past a continuously moving plate with suction or injection, The Korean Society for Industrial and Aapplied Mathematics, 2005

[14] G C Hazarika, US Gopal Ch., Effects of variable viscosity and thermal conductivity on MHD flow past a vertical plate, Matem´aticas, Vol. xx, No 2, pp. 45-54, 2012.

[15] C. Ozalp, Entropy generation for nonisothermal fluid flow: Variable thermal conductivity and viscosity case, Adv. in Mech. Engg., Vol. 2013, Article ID 797894, 9 pages, 2013.

[16] NC Mahanti, P Gaur, Effects of varying viscosity and thermal conductivity on steady free convective flow and heat transfer along an isothermal vertical plate in the presence of heat sink, J. of Appl. Fluid Mech., Vol. 2, No. 1, pp. 23-28, 2009.

[17] PR Sharma and G Singh, Effects of variable thermal conductivity and heat source / sink on MHD flow near a stagnation point on a linearly stretching sheet, J. of Appl. Fluid Mech., Vol. 2, No. 1, pp. 13-21, 2009.

[18] M. Choudhury and GC Hazarika, The effects of variable viscosity and thermal conductivity on mhd flow due to a point sink, Matem´aticas, Vol. xvi, No 2, pp. 21-28, 2008.

[19] R Nasrin, Influences of physical parameters on mixed convection in a horizontal lid driven cavity with undulating base surface, Num. Heat Trans., Part A-Applications, Vol. 61, pp. 306-321, 2012.

[20] R Nasrin, MA Alim and AJ Chamkha, Combined convection flow in triangular wavy chamber filled with water-CuO nanofluid: Effect of viscosity models, Int. Commun. in Heat and Mass Transf., 39 (8), 1226-1236, 2012.

[21] KC Lin, A Violi, Natural convection heat transfer of nanofluids in a vertical cavity: Effects of non-uniform particle diameter and temperature on thermal conductivity, Int. J. of Heat and Fluid Flow, Vol. 31, pp. 236-245, 2010.

[22] J Charraudeau, Influence de gradients de properties physiques en convection force application au cas du tube, Int. J. of Heat and Mass Transf., Vol. 18, pp. 87-95, 1975.

[23] MA Hossain, MS Munir, DAS Rees, Flow of viscous incompressible fluid with temperature dependent viscosity and thermal conductivity past a permeable wedge with uniform surface heat flux, Int. J. Therm. Sci., Vol. 39, pp. 635-644, 2000.

[24] HC Brinkman, The viscosity of concentrated suspensions and solution, J. Chem. Phys., Vol. 20, pp. 571–581, 1952.

[25] JC Maxwell-Garnett, Colours in metal glasses and in metallic films, Philos. Trans. Roy. Soc. A, Vol. 203, pp. 385–420, 1904.

[26] C Taylor, P Hood, A numerical solution of the Navier-Stokes equations using finite element technique, Computer and Fluids, Vol. 1, pp. 73–89, 1973.

[27] P Dechaumphai, Finite Element Method in Engineering, 2nd ed., Chulalongkorn University Press, Bangkok, 1999.

[28] EB Ogut, Natural convection of water-based nanofluids in an inclined enclosure with a heat source, Int. J. of Thermal Sciences, Vol. 48, pp. 1–11, 2009.

NOMENCLATURE

A Area of nanofluid layer (m^2)

A_m Dimensionless amplitude of wave

C_p Specific heat at constant pressure (J kg^{-1} K^{-1})

g Gravitational acceleration (m s^{-2})

h Local heat transfer coefficient (W m^{-2} K^{-1})

H Height of the nanofluid layer (m)

k Thermal conductivity (W m^{-1} K^{-1})

L Length of the thin layer (m)

Nu Nusselt number, $Nu = hL/k_f$

Pr Prandtl number, $Pr = \nu_f / \alpha_f$

Ra Rayleigh number, $Ra = \dfrac{g\beta_f L^3 (T_w - T_c)}{\nu_f \alpha_f}$

T Dimensional temperature (K)

u, v Dimensional x and y components of velocity (m s^{-1})

U, V Dimensionless velocities, $U = \dfrac{uL}{\nu_f}$, $V = \dfrac{vL}{\nu_f}$

V Magnitude of dimensionless velocity

X, Y Dimensionless coordinates, $X = x/L$, $Y = y/L$

x, y Dimensional coordinates (m)

Greek Symbols

α Fluid thermal diffusivity (m^2 s^{-1})

β Thermal expansion coefficient (K^{-1})

θ Dimensionless temperature, $\theta = (T - T_c)/(T_w - T_c)$

λ Number of wave

μ Dynamic viscosity (N s m^{-2})

ν Kinematic viscosity (m^2 s^{-1})

ρ Density (kg m^{-3})

ϕ Nanoparticles volume fraction

Subscripts

av average

c cold

f fluid

nf nanofluid

s solid nanoparticle

w top wall